

ARMY RESEARCH LABORATORY



A Study of the Phase-Lock Phenomenon for a Circular Slingatron

by Gene R. Cooper and Derek A. Tidman

ARL-TR-2566

September 2001

Approved for public release; distribution is unlimited.

20011005 371

The findings in this report are not to be construed as an official Department of the Army position unless so designated by other authorized documents.

Citation of manufacturer's or trade names does not constitute an official endorsement or approval of the use thereof.

Destroy this report when it is no longer needed. Do not return it to the originator.

Army Research Laboratory

Aberdeen Proving Ground, MD 21005-5066

ARL-TR-2566

September 2001

A Study of the Phase-Lock Phenomenon for a Circular Slingatron

Gene R. Cooper

Weapons and Materials Research Directorate, ARL

Derek A. Tidman

ALCorp.

Approved for public release; distribution is unlimited.

Abstract

The phase-lock phenomenon of a mass sled sliding along in a circular slingatron is studied both numerically and analytically. Parameters that describe a slingatron, in which the phase angle of the swing arms increases quadratically in time, are found to be simply related to the sled's speed during phase lock. The time required for phase lock to occur is related to a simple exponential function of the gyration speed and the coefficient of friction between the sled and track. Accurate time histories describing the motion of the accelerating sled are expressed in terms of confluent hypergeometric functions ${}_1F_1$. These results are then used to obtain physical insight into why the phase-lock phenomenon takes place and to describe the important role that friction plays by damping the oscillatory motion of the sled.

Contents

List of Figures	v
1. Introduction	1
2. Equations of Motion	1
3. Phase Lock In	3
4. Driven Circular Slingatron	4
5. Conclusions	10
6. References	11
List of Symbols	13
Distribution List	15
Report Documentation Page	17

INTENTIONALLY LEFT BLANK.

List of Figures

Figure 1. Schematic of a circular slingatron.....	2
Figure 2. Divergent velocity for $R = 5$ m, $t_{\infty} = 2.68$ s.	4
Figure 3. Velocity vs. time $P = \dot{f} / f^2$, $\alpha = r/R$	5
Figure 4. Angle lock in vs. time $P = \dot{f} / f^2$, $\alpha = r/R$	5
Figure 5. Comparison of numerical vs. analytical results.....	9
Figure 6. Comparison of velocities for $\dot{f} / f = 1/250$	9
Figure 7. Comparison of velocities with and without damping $\mu \neq 0$, $\mu = 0$	10

INTENTIONALLY LEFT BLANK.

1. Introduction

A concept called the slingatron, used to accelerate a mass (sled) to high velocity, has been proposed and studied by Tidman [1]. This accelerator can propel either a constant mass or an ablating mass sled along a guide tube forming the slingatron track [2]; several slingatron configurations have been examined [1, 2]. A simple friction model is also used in which the friction force is assumed to be proportional to the normal force exerted by the track [2] on the moving sled.

Previous work has shown that the relative phase angle (between the sleds' velocity vector and the gyration velocity vector of the guide tube) locks into an approximate constant value. This report presents numerical and analytical results found from our investigation of this phase-lock phenomenon for a constant point mass accelerated around a circular track with the friction coefficient taken to be a constant. Numerical simulations, as well as simple analytical results, show that the mass can reach very high velocities, provided that the gyration speed can increase with sufficient acceleration. We will show that when the gyration phase angle varies quadratically with time, the phase-lock value plus the time required to obtain this value are simply related to the gyration acceleration, the coefficient of friction, and the ratio of the two characteristic lengths that describes the slingatron geometry. These relationships are used to aid our understanding and to make predictions of the phase-lock phenomenon.

2. Equations of Motion

Consider the circular slingatron shown in Figure 1, which has radius vector \mathbf{R} at the sled location with its center attached to the gyration arm \mathbf{r} positioned at angle $\psi(t)$ with respect to the laboratory frame at time t . The position of the accelerating point mass is given by $\mathbf{R} + \mathbf{r}$, and the corresponding velocity is therefore $\mathbf{V} = \dot{\mathbf{R}} + \dot{\mathbf{r}}$. The force \mathbf{F} acting on the mass M can be written as $\mathbf{F} = F_{\perp} \mathbf{m} + F_{\parallel} \mathbf{n}$, in which $\mathbf{m} = \mathbf{n} \times \mathbf{k}$ and $\mathbf{n} = -\mathbf{R}'/R'$ are unit vectors pointing normal (toward the center of the circle) and anti-parallel to the circular track. Letting \mathbf{i}, \mathbf{j} be unit vectors along the laboratory frame's abscissa and ordinate gives the time derivative of the momentum equations the following form:

$$M\ddot{x} = -F_{\perp} \cos\phi + F_{\parallel} \sin\phi \quad \text{and} \quad M\ddot{y} = -F_{\perp} \sin\phi - F_{\parallel} \cos\phi, \quad (1)$$

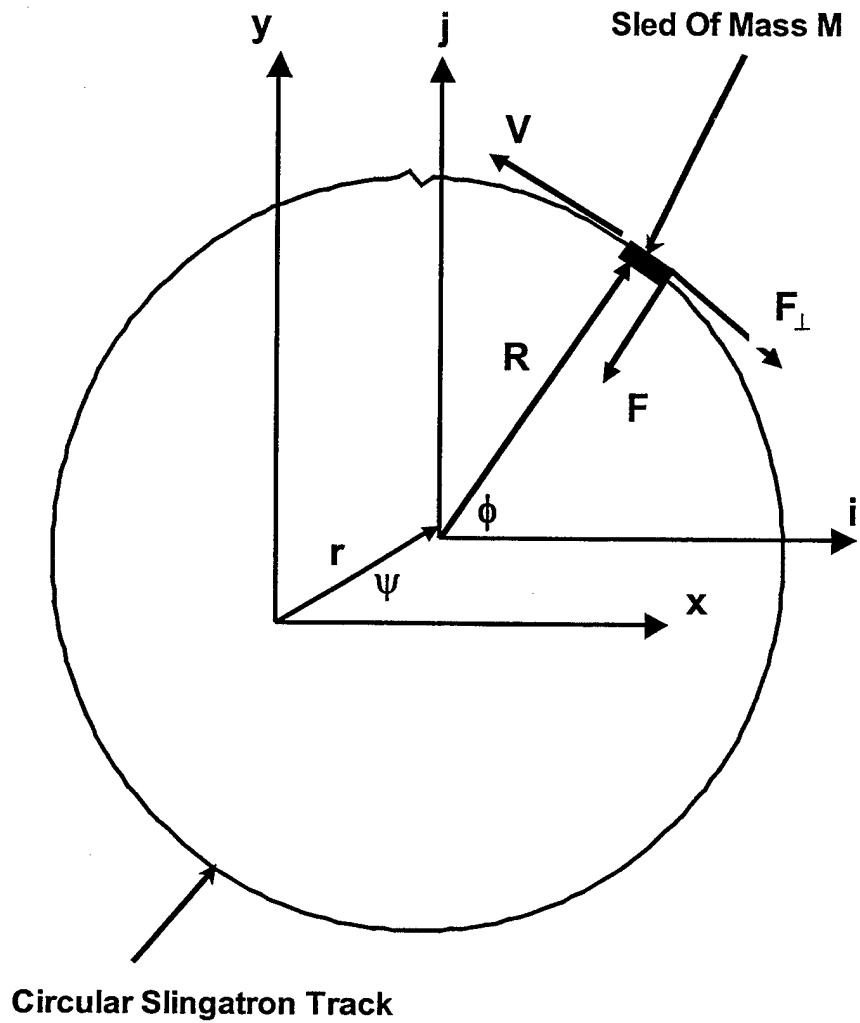


Figure 1. Schematic of a circular slingatron.

with Cartesian coordinates (x, y) in the (\mathbf{i}, \mathbf{j}) laboratory frame constrained so that

$$x = R\cos\phi + r\cos\psi \quad \text{and} \quad y = R\sin\phi + r\sin\psi . \quad (2)$$

The parallel the force, $F_{//}$, attributed to friction is represented as

$$F_{//} = \mu F_{\perp} . \quad (3)$$

Equations (1-3) will determine the angle ϕ in terms of the given angle $\psi(t)$ resulting from the following differential equation

$$-\ddot{\phi} = \mu \dot{\phi}^2 + \alpha (\ddot{\psi} + \mu \dot{\psi}^2) \cos(\psi - \phi) + \alpha (\mu \ddot{\psi} - \dot{\psi}^2) \sin(\psi - \phi) \quad (4)$$

for which the length ratio is defined as $\alpha = r/R$.

Generally, the solution to equation (4) is obtained from numerical integration for any choice of the time-dependent gyration angle $\psi(t)$. The mass velocity $V^2 = \dot{x}^2 + \dot{y}^2$ relative to the laboratory reference frame is easily calculated using

$$V^2 = \left[2\alpha \cos(\psi - \phi) \frac{\dot{\phi}}{\dot{\psi}} + \alpha^2 + \left(\frac{\dot{\phi}}{\dot{\psi}} \right)^2 \right] \dot{\psi}^2 R^2. \quad (5)$$

3. Phase Lock In

Tidman [1] has presented a complete analysis of cases where phase lock in occurs for all times, t , when the angle $\theta = \psi - \phi$ is constant, so that $\dot{\phi} = \dot{\psi}$ and $\ddot{\phi} = \ddot{\psi}$. These conditions transform equation (4) to

$$\ddot{\phi} = b \dot{\phi}^2, \quad b = \frac{\alpha (\sin \theta - \mu \cos \theta) - \mu}{\alpha (\mu \sin \theta + \cos \theta) + 1}, \quad (6)$$

and this is easily integrated so that equation (5) becomes

$$V^2 = \frac{(\dot{\phi}_0 R)^2 (2\alpha \cos \theta + \alpha^2 + 1)}{(b \dot{\phi}_0 t - 1)^2} \quad (7)$$

with $\phi_0 = \phi(0)$ and $\dot{\phi}_0 = \dot{\phi}(0)$.

Examining the factor b , defined in the second equation of equations (6), shows that the velocity is time independent when $b = 0$ so the parameters are related as

$$\theta = \pm 2 \tan^{-1} \left[\frac{\sqrt{(\alpha^2 - 1)\mu^2 + \alpha^2} \pm \alpha}{(\alpha - 1)\mu} \right] \pm n\pi, \quad n = 0, 1, 2, \dots, \quad (8)$$

so that

$$V^2 = \frac{(1 \pm \sqrt{(\alpha^2 - 1)\mu^2 + \alpha^2})^2 (\dot{\phi}_0 R)^2}{\mu^2 + 1}.$$

A short amount of algebra reveals that equation (8) is satisfied whenever the force caused by friction, μF_{\perp} , is large enough to prevent the point mass from accelerating in a direction tangent to the circular track. Furthermore, the velocity given by equation (7) was shown by Tidman [1] to diverge (to a nonrelativistic limit) at the time $t_{\infty} = (\dot{\phi}_0 b)^{-1}$. In practice, for this to occur, one must have $t_{\infty} \geq 0$, which means that a divergent velocity V will occur under the

assumption $\alpha\sqrt{1+\mu^2} \leq 1$, whenever the parameters also satisfy the relation

$$\sin(\theta - \tan^{-1} \mu) \geq \frac{\mu}{\alpha\sqrt{\mu^2 + 1}}. \quad (9)$$

An example typical of this behavior is shown in Figure 2.

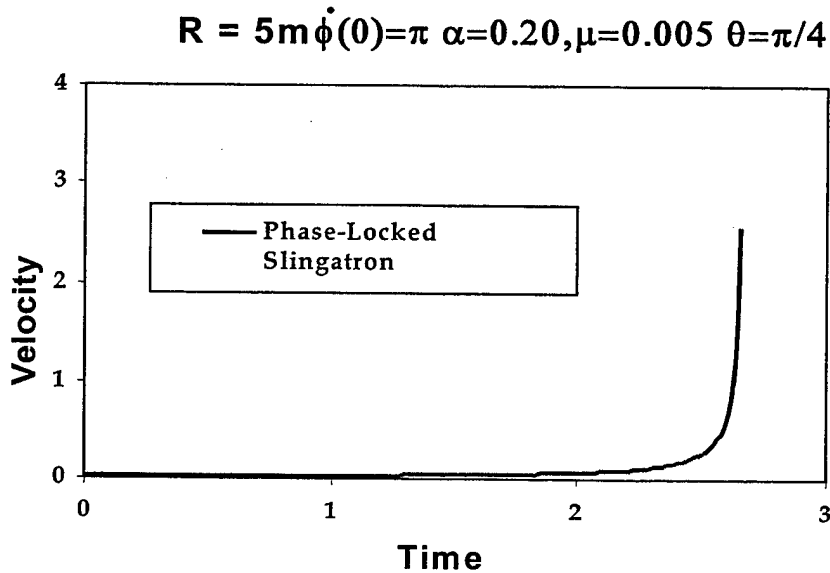


Figure 2. Divergent velocity for $R = 5 \text{ m}$, $t_0 = 2.68 \text{ s}$.

4. Driven Circular Slingatron

We next consider a class of slingatrons so that the gyration of the circular track is prescribed by the angular displacement $\psi(t) = \psi_0 + 2\pi f t + \pi \dot{f} t^2$ for constants f and \dot{f} . Typical numerical solutions to equation (4) and equation (5) are given in Figure 3 with initial conditions $\phi_0 = 0$ and $\phi_0 = 2\pi f$. Two corresponding calculations of the angle $\theta = \psi - \phi$ as functions of time are shown in Figure 4. The last two plots show that the slingatron will eventually achieve phase lock in, i.e. $\dot{\theta} = 0$ and $\ddot{\theta} = 0$, when the gyration angle is quadratic in time, i.e. $\psi(t) = \psi_0 + 2\pi f t + \pi \dot{f} t^2$.

To better understand how the final lock-in angle is related to the given parameters, we now rewrite equation (4) in terms of $\theta = \psi - \phi$ and calling $q = \dot{f} t + f$ we get

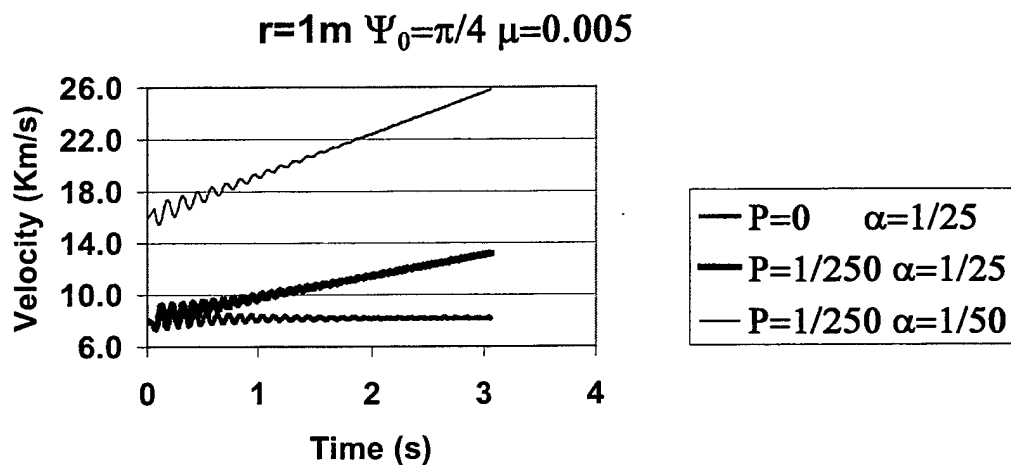


Figure 3. Velocity vs. time $P = \dot{f} / f^2, \alpha = r/R$.

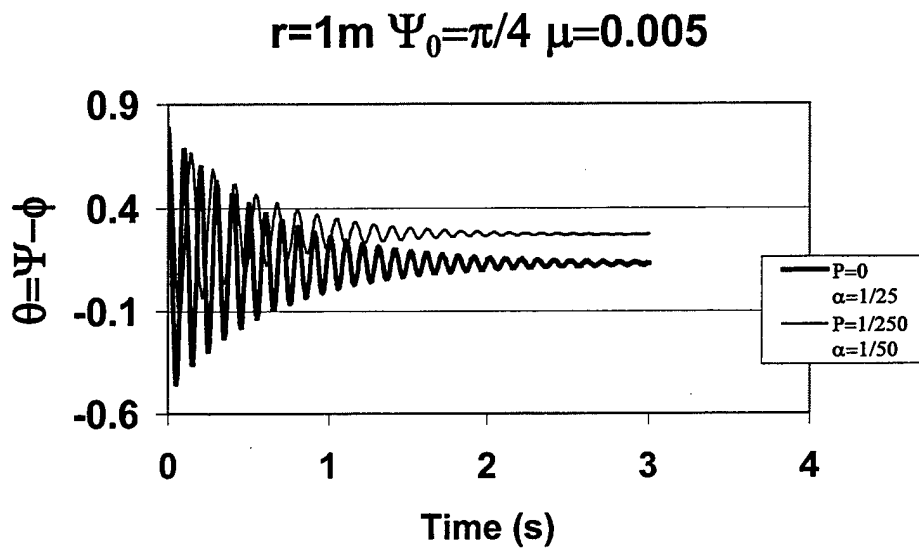


Figure 4. Angle lock in vs. time $P = \dot{f} / f^2, \alpha = r/R$.

$$\begin{aligned} \dot{f}^2 \theta'' - \dot{f}^2 \mu \theta'^2 + 4\pi \mu q \theta' + 2\pi \alpha (2\pi q^2 - \dot{f} \mu) \sin \theta - \\ 2\pi \alpha (2\pi q^2 + \dot{f}) \cos \theta = 2\pi (\pi \mu q^2 + \dot{f}). \end{aligned} \quad (10)$$

Focusing our attention on large values of t , consider the following asymptotic expansion for θ

$$\theta = \theta_0 + \frac{\theta_2}{q^2} + \frac{\theta_4}{q^4} + \frac{\theta_6}{q^6} + \dots$$

Substituting this back into equation (10) and keeping only the largest order term gives us

$$\begin{aligned} 4\pi^2 [\alpha \sin(\theta_0) - \alpha \mu \cos(\theta_0) - \mu] = 0 \Rightarrow \\ \lim_{t \rightarrow \infty} \frac{\theta_0}{2} \rightarrow \tan^{-1} \left[\frac{-\alpha \pm \sqrt{\alpha^2 + \mu^2 (\alpha^2 - 1)}}{\mu (\alpha^2 - 1)} \right] + n\pi, \quad n = 0, 1, 2, \dots \end{aligned}$$

However, Tidman [1] has shown that θ values near to $\pi/2$ lead to instabilities, which tells us that the correct asymptotic must have the following form

$$\begin{aligned} \lim_{t \rightarrow \infty} \frac{\theta_0}{2} \rightarrow 2n\pi + \tan^{-1} \left[\frac{-\alpha + \sqrt{\alpha^2 + \mu^2 (\alpha^2 - 1)}}{\mu (\alpha^2 - 1)} \right] \approx \\ \frac{(\alpha + 1)\mu}{\alpha} + O(\mu^3), \quad n = 0, 1, \dots \end{aligned} \quad (11)$$

The limiting value plotted in Figure 4 corresponds to equation (11) with $n = 0$. Subtracting this asymptotic value of θ so that $\gamma \rightarrow \theta + \theta_0$ transforms equation (10) (after some algebra) to the following expression:

$$\begin{aligned} \dot{f}^2 \gamma'' - \mu \dot{f}^2 \gamma'^2 + 4\pi \mu \dot{f} q \gamma' + 2\pi (2\pi \lambda q^2 + \dot{f} \mu) \sin \gamma + \\ 2\pi (2\pi \mu q^2 - \dot{f} \lambda) \cos \gamma = 2\pi (\mu \pi q^2 + \dot{f}), \end{aligned} \quad (12)$$

$$\lambda = \sqrt{(\alpha^2 - 1)\mu^2 + \alpha^2}, \quad q = \dot{f} t + f.$$

Since $\theta_0 \approx \mu + \mu/\alpha$ is small for realistic values of μ and α , we now make the small angle approximation, $\gamma \ll 1$, reducing equation (12) to

$$\begin{aligned} \dot{f}^2 \gamma'' + 4\pi \dot{f} \mu q \gamma' + 2\pi (2\pi \lambda q^2 + \dot{f} \mu) \gamma = 2\pi (\dot{f} \lambda + 1) \\ \gamma(f) = \psi_0 - \theta_0 \quad \text{and} \quad \dot{\gamma}(f) = 0. \end{aligned} \quad (13)$$

There are many ways to write solutions to equation (13), but we use the following procedure, which seemed expedient for both numerical and analytic examinations. First, make the substitutions

$$\begin{aligned}\rho &= 2\Gamma q^2/\dot{f} \\ z &= \gamma \exp\left((\pi\mu + \Gamma)q^2/\dot{f}\right)\end{aligned}\quad (14)$$

into the left-hand side of equation (13), which gives us,

$$\rho z'' + \left(\frac{1}{2} - \rho\right)z' + \frac{\rho(\pi^2\lambda^2 + \Gamma - \pi^2\mu) - \Gamma^2}{4\Gamma^2}z = 0.$$

Next, choose $\Gamma = \pm i\pi\sqrt{\lambda - \mu^2}$ to force the coefficient of z to be independent of ρ so that the left-hand side of equation (13) is now transformed into the complex plane such that

$$\rho z'' + \left(\frac{1}{2} - \rho\right)z' - z/4 = 0. \quad (15)$$

The solution to equation (15) is a linear combination of the confluent hypergeometric function [3], ${}_1F_1$, so the solution of the left-hand side of equation (13), γ_H , is

$$\begin{aligned}\gamma_H(\rho) &= \left[C1 {}_1F_1\left(\frac{1}{4}, \frac{1}{2}, \rho\right) + C2 \sqrt{\rho} {}_1F_1\left(\frac{3}{4}, \frac{3}{2}, \rho\right) \right] \\ &\times \exp\left[\left(i\sqrt{\lambda - \mu^2} - \mu\right)\pi q^2/\dot{f}\right], \lambda - \mu^2 > 0,\end{aligned}\quad (16)$$

for complex constants $C1, C2$. Inspecting equation (13) reveals that the complex conjugate of equations (14) will cause equation (15) to be replaced by its conjugate. Thus, the conjugate of equation (16) will also produce equally valid solutions, γ_H^* , to equation (13). The required real values of γ are now found by taking linear combinations (average values) of γ_H and γ_H^* .

These results show that the amplitude of γ and therefore θ decrease as the factors

$$\left\{ \begin{array}{c} \dot{f}t + f \\ 1 \end{array} \right\} \exp\left(-\pi\mu(\dot{f}t + f)^2/\dot{f}\right), \quad (17)$$

provided that the functions ${}_1F_1$ for the parameters used here do not diverge. This is easily shown by the use of the integral representation [3] of ${}_1F_1$,

$${}_1F_1(1/4, 1/2, \rho) = \frac{\sqrt{\pi}}{\Gamma(1/4)\Gamma(1/4)} \int_0^1 t^{-3/4} e^{\rho t} (1-t)^{-3/4} dt. \quad (18)$$

Now taking the absolute value of each side of equation (18) and remembering that ρ is purely imaginary, we find

$$\begin{aligned}
|{}_1F_1(1/4, 1/2, \rho)| &= \left| \frac{\sqrt{\pi}}{\Gamma(1/4)\Gamma(1/4)} \right| \left| \int_0^1 t^{-3/4} e^{\rho t} (1-t)^{-3/4} dt \right| \\
&\leq \frac{\sqrt{\pi}}{\Gamma(1/4)^2} \int_0^1 t^{-3/4} (1-t)^{-3/4} dt \\
&= 1,
\end{aligned} \tag{19}$$

showing that ${}_1F_1(1/4, 1/2, \rho)$ is bound; a similar argument shows that ${}_1F_1(1/4, 3/2, \rho)$ is also bound. Thus, the homogeneous solutions, given by equation (16), decay according to equation (17). Obtaining solutions for the limiting case, in which $f \rightarrow 0$, is easily performed directly from the first of equations (13). For this case, the solution θ has the form

$$\theta = \left[C1 \cos\left(2\pi f \sqrt{\alpha - \mu^2 t}\right) + C2 \sin\left(2\pi f \sqrt{\alpha - \mu^2 t}\right) \right] \exp(-2\pi f \mu t), \tag{20}$$

which shows that the decaying factors of equations (17) are replaced with $\exp(-2\pi f \mu t)$.

The nonhomogeneous solution of equation (13) can be shown to asymptotically approach zero for large t . Therefore, the asymptotic solution found in equation (11) continues to show $\theta \rightarrow \theta_0 \approx \mu + \mu/\alpha$ for small values of μ and α . A sample from Figure 4 that exhibits both the asymptotic and decaying characteristics of a solution to equation (13) is given in Figure 5. The velocity corresponding to the asymptotic solution of equation (13) can be obtained from equation (5) by letting $\phi/\psi \rightarrow 1$. Thus, one will find

$$V \rightarrow \frac{\sqrt{(\alpha^2 - 1)\mu^2 + \alpha^2} + 1}{\sqrt{\mu^2 + 1}} R\dot{\psi} \approx \frac{(\alpha + 1)(2\alpha - \mu^2)}{\alpha} R\dot{\psi}, \tag{21}$$

and this shows that velocity is asymptotically proportional to $R\dot{\psi}$ for our choice of ψ . Choosing $f = 0$, one will find that the asymptotic solution to equation (10) will now contain both even and odd powers of t , but the 0-th order term will still have the solution given by equations (11).

Equation (6) and the long time limit found in equations (11) tell us that $b \rightarrow 0$, which implies $t_\infty = (b\dot{\phi}_0)^{-1} \rightarrow \infty$. Thus, the sled will continue to gain velocity for a long period of time whenever the gyration speed varies quadratically with t . An example of this is given in Figure 6, which shows that both the numerical and the analytical results are in good agreement, again providing compelling evidence for the decaying factors given in equation (17) as well as the value as the final phase-lock angle.

So far, we have assumed that the friction coefficient is very small but finite $0 < \mu \ll \alpha < 1$. Equations (17) and (20) show that friction plays a very important role in that it is responsible for damping out the oscillations of the

$r=1\text{m}$ $\Psi_0=\pi/4$ $\mu=0.005$ $P=1/250$ $\alpha=1/50$

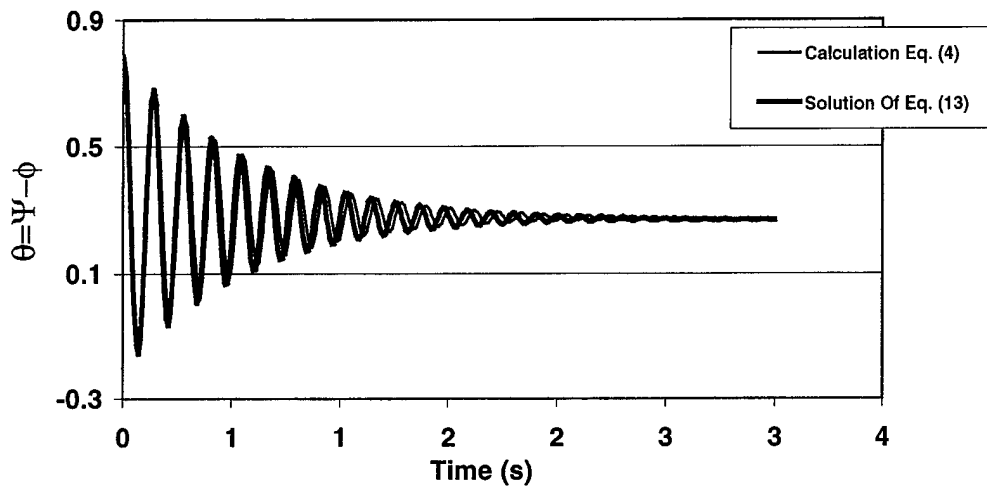


Figure 5. Comparison of numerical vs. analytical results.

$r=1\text{m}$ $\alpha=0.20$ $\Psi_0=\pi/4$ $\mu=0.0050$

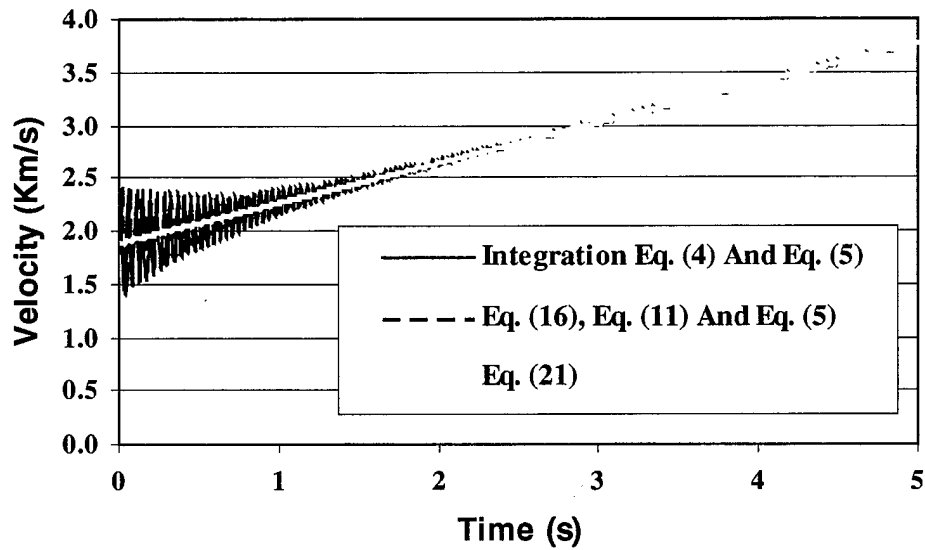


Figure 6. Comparison of velocities for $\hat{f}/f = 1/250$.

mass sled as it progresses along the circular track. Setting $\mu = 0$ in equations (11) and (21) shows that the long time limits for θ and V become $2n\pi$ and $(\alpha + 1)\dot{\psi}$, respectively. Figure 7 displays the influence of friction where one can see that the velocity no longer damps to the asymptotic limit, $V = (\alpha + 1)\dot{\psi}$, when the force attributed to friction is assumed to be zero.

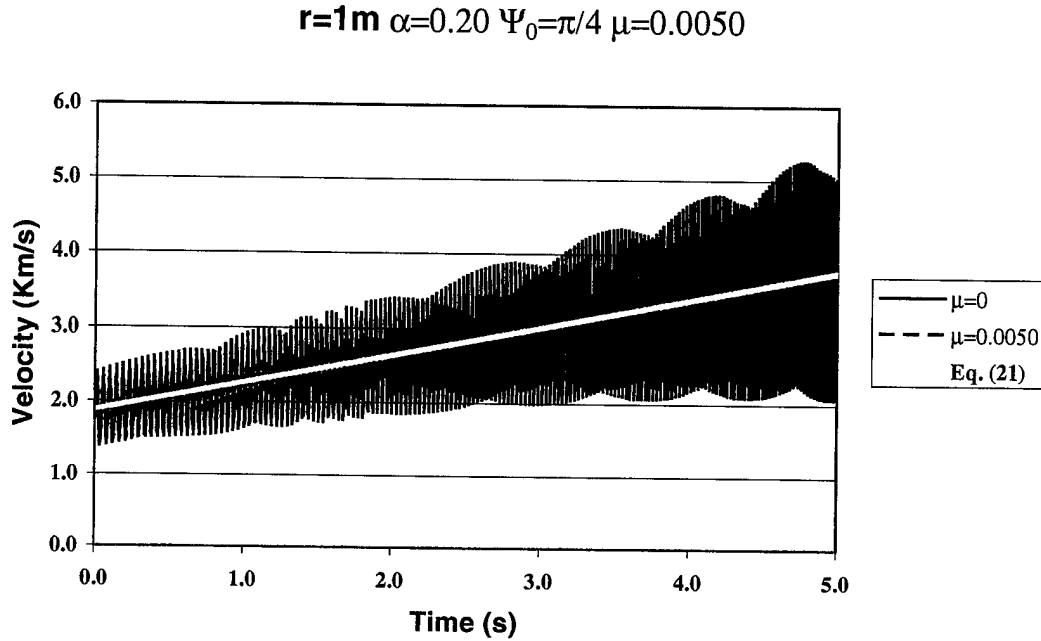


Figure 7. Comparison of velocities with and without damping $\mu \neq 0, \mu = 0$.

5. Conclusions

The analysis presented here gives an explicit expression for the rate at which an accelerating mass becomes phase locked while it traverses a circular slingatron having a gyration phase angle ψ varying as a quadratic with time. We have also shown that the final phase-lock angle has the simple expression $\theta \rightarrow \mu + \mu/\alpha$ for the usual small values of μ and α . In order to keep θ constant, we must gradually increase ψ so that it diverges at $t = (b\dot{\psi}_0)^{-1}$, as does the phase-locked ϕ . This is because as the gyration speed $2\pi R(\dot{\psi} t + \dot{\psi})$ increases, so must the mass gain speed $\approx 2\pi \alpha \sin(\theta)$ (see equation [5] for $\theta = \text{constant}$) per turn. However, we choose, $\psi = \psi_0 + 2\pi f t + \pi \dot{f} t^2$, which causes the gyration speed to become large at large times. Thus, we have shown that the only way the mass can stay phase locked with this increasing gyration speed is to assume smaller values of θ so that it does not gain too much velocity per turn. For our choice of ψ , we have $\theta \rightarrow \mu + \mu/\alpha \ll 1$, as time becomes large, thus keeping the accelerating mass phase locked with gyration.

6. References

1. Tidman, D. A. "Slingatron Mass Launchers." *Journal of Propulsion and Power*, vol. 14, pp. 537-544, July-August 1998.
2. Cooper, G. R., and D. A. Tidman. "Numerical Simulations of the Slingatron." *AIAA Journal of Propulsion and Power*, to be published.
3. U.S. Department of Commerce. *Handbook of Mathematical Functions with Formulas, Graphs, and Mathematical Tables*. Applied Mathematics Series 55 (AMS-55), National Bureau of Standards, 1964.

INTENTIONALLY LEFT BLANK.

List of Symbols

a	=	complex parameter for the confluent hypergeometric function ${}_1F_1$
b	=	constant of integration
$C1, C2$	=	complex constants of integration
f	=	frequency of gyration arm $1/s$
\dot{f}	=	angular acceleration of gyration arm $1/s^2$
$\mathbf{F}_{//}$	=	force vector parallel to slingatron track $ \mathbf{F}_{//} = F_{//}$
\mathbf{F}_{\perp}	=	force vector perpendicular to slingatron track $ \mathbf{F}_{\perp} = F_{\perp}$
${}_1F_1$	=	confluent hypergeometric function
i	=	$\sqrt{-1}$
\mathbf{i}	=	unit vector along ordinate
\mathbf{j}	=	unit vector along abscissa
\mathbf{k}	=	unit vector $\mathbf{k} = \mathbf{i} \times \mathbf{j}$
M	=	mass of slingatron sled
P	=	frequency ratio $= \dot{f}/f^2$
q	=	transform of independent variable
\mathbf{R}	=	radius vector of slingatron circle
\mathbf{r}	=	radius vector of gyration arm $ \mathbf{r} = r$
t	=	time
\mathbf{V}	=	velocity vector $V = \sqrt{\dot{x}^2 + \dot{y}^2}$
\hat{V}	=	velocity of sled relative to the track
x	=	ordinate of sled
y	=	abscissa of sled
z	=	transformed dependent variable
α	=	ratio of radii r/R
γ	=	polar angle
μ	=	coefficient of friction
ρ	=	transformed independent variable

ϕ	=	polar angle of vector R
ψ	=	polar angle of vector r
θ	=	lock-in angle = $\psi - \phi$
$ $	=	absolute value
$(\dot{})$	=	$\frac{d}{dt}$
(\prime)	=	$\frac{d}{dq}, \frac{d}{d\rho}, \frac{d}{d\phi}$
O	=	order of magnitude
*	=	complex conjugate

<u>NO. OF COPIES</u>	<u>ORGANIZATION</u>
2	DEFENSE TECHNICAL INFORMATION CENTER DTIC OCA 8725 JOHN J KINGMAN RD STE 0944 FT BELVOIR VA 22060-6218
1	HQDA DAMO FDT 400 ARMY PENTAGON WASHINGTON DC 20310-0460
1	OSD OUSD(A&T)/ODDR&E(R) DR R J TREW 3800 DEFENSE PENTAGON WASHINGTON DC 20301-3800
1	COMMANDING GENERAL US ARMY MATERIEL CMD AMCRDA TF 5001 EISENHOWER AVE ALEXANDRIA VA 22333-0001
1	INST FOR ADVNCD TCHNLGY THE UNIV OF TEXAS AT AUSTIN 3925 W BRAKER LN STE 400 AUSTIN TX 78759-5316
1	DARPA SPECIAL PROJECTS OFFICE J CARLINI 3701 N FAIRFAX DR ARLINGTON VA 22203-1714
1	US MILITARY ACADEMY MATH SCI CTR EXCELLENCE MADN MATH MAJ HUBER THAYER HALL WEST POINT NY 10996-1786
1	DIRECTOR US ARMY RESEARCH LAB AMSRL D DR D SMITH 2800 POWDER MILL RD ADELPHI MD 20783-1197

<u>NO. OF COPIES</u>	<u>ORGANIZATION</u>
1	DIRECTOR US ARMY RESEARCH LAB AMSRL CI AI R 2800 POWDER MILL RD ADELPHI MD 20783-1197
3	DIRECTOR US ARMY RESEARCH LAB AMSRL CI LL 2800 POWDER MILL RD ADELPHI MD 20783-1197
3	DIRECTOR US ARMY RESEARCH LAB AMSRL CI IS T 2800 POWDER MILL RD ADELPHI MD 20783-1197
	<u>ABERDEEN PROVING GROUND</u>
2	DIR USARL AMSRL CI LP (BLDG 305)

INTENTIONALLY LEFT BLANK.

REPORT DOCUMENTATION PAGE			Form Approved OMB No. 0704-0188	
Public reporting burden for this collection of information is estimated to average 1 hour per response, including the time for reviewing instructions, searching existing data sources, gathering and maintaining the data needed, and completing and reviewing the collection of information. Send comments regarding this burden estimate or any other aspect of this collection of information, including suggestions for reducing this burden, to Washington Headquarters Services, Directorate for Information Operations and Reports, 1215 Jefferson Davis Highway, Suite 1204, Arlington, VA 22202-4302, and to the Office of Management and Budget, Paperwork Reduction Project(0704-0188), Washington, DC 20503.				
1. AGENCY USE ONLY (Leave blank)		2. REPORT DATE September 2001	3. REPORT TYPE AND DATES COVERED Final, November 2000 – February 2001	
4. TITLE AND SUBTITLE A Study of the Phase-Lock Phenomenon for a Circular Slingatron			5. FUNDING NUMBERS 1L162618.AH80	
6. AUTHOR(S) Gene R. Cooper and Derek A. Tidman*				
7. PERFORMING ORGANIZATION NAME(S) AND ADDRESS(ES) U.S. Army Research Laboratory ATTN: AMSRL-WM-BC Aberdeen Proving Ground, MD 21005-5066			8. PERFORMING ORGANIZATION REPORT NUMBER ARL-TR-2566	
9. SPONSORING/MONITORING AGENCY NAMES(S) AND ADDRESS(ES)			10. SPONSORING/MONITORING AGENCY REPORT NUMBER	
11. SUPPLEMENTARY NOTES *ALCorp., 6801 Benjamin Street, McLean, VA 22101				
12a. DISTRIBUTION/AVAILABILITY STATEMENT Approved for public release; distribution is unlimited.			12b. DISTRIBUTION CODE	
13. ABSTRACT (Maximum 200 words) The phase-lock phenomenon of a mass sled sliding along in a circular slingatron is studied both numerically and analytically. Parameters that describe a slingatron, in which the phase angle of the swing arms increases quadratically in time, are found to be simply related to the sled's speed during phase lock. The time required for phase lock to occur is related to a simple exponential function of the gyration speed and the coefficient of friction between the sled and track. Accurate time histories describing the motion of the accelerating sled are expressed in terms of confluent hypergeometric functions ${}_1F_1$. These results are then used to obtain physical insight into why the phase-lock phenomenon takes place and to describe the important role that friction plays by damping the oscillatory motion of the sled.				
14. SUBJECT TERMS slingatron, mass accelerator, friction, speed, gyration, lock-in, phase lock			15. NUMBER OF PAGES 19	
			16. PRICE CODE	
17. SECURITY CLASSIFICATION OF REPORT UNCLASSIFIED	18. SECURITY CLASSIFICATION OF THIS PAGE UNCLASSIFIED	19. SECURITY CLASSIFICATION OF ABSTRACT UNCLASSIFIED	20. LIMITATION OF ABSTRACT UL	

INTENTIONALLY LEFT BLANK.